Combined Small Interfering RNA Therapy and In Vivo Magnetic Resonance Imaging in Islet Transplantation

Combined Small Interfering RNA Therapy and In Vivo Magnetic Resonance Imaging in Islet Transplantation

Ping Wang,[1] Mehmet V. Yigit,[1] Zdravka Medarova,[1] Lingling Wei,[2] Guangping Dai,[1] Christian Schuetz,[2] and Anna Moore[1]

OBJECTIVE—Recent advances in human islet transplantation are hampered by significant graft loss shortly after transplantation and inability to follow islet fate directly. Both issues were addressed by utilizing a dual-purpose therapy/imaging small interfering RNA (siRNA)-nanoparticle probe targeting apoptotic-related gene caspase-3. We expect that treatment with the probe would result in significantly better survival of transplanted islets, which could be monitored by in vivo magnetic resonance imaging (MRI).

RESEARCH DESIGN AND METHODS—We synthesized a probe consisting of therapeutic (siRNA to human caspase-3) and imaging (magnetic iron oxide nanoparticles, MN) moieties. In vitro testing of the probe included serum starvation of the islets followed by treatment with the probe. Caspase-3 gene silencing and protein expression were determined by RT-PCR and Western blot, respectively. In vivo studies included serial MRI of NOD-SCID mice transplanted with MN-small interfering (si)Caspase-3–labeled human islets under the left kidney capsule and MN-treated islets under the right kidney capsule.

RESULTS—Treatment with MN-siCaspase-3 probe resulted in decrease of mRNA and protein expression in serum-starved islets compared with controls. In vivo MRI showed that there were significant differences in the relative volume change between MN-siCaspase-3–treated grafts and MN-labeled grafts. Histology revealed decreased caspase-3 expression and cell apoptosis in MN-siCaspase-3–treated grafts compared with the control side.

CONCLUSIONS—Our data show the feasibility of combining siRNA therapy and in vivo monitoring of transplanted islets in mice. We observed a protective effect of MN-siCaspase-3 in treated islets both in vitro and in vivo. This study could potentially aid in increasing the success of clinical islet transplantation. ***Diabetes*** **60:565–571, 2011**

Type 1 diabetes results from a T-cell–mediated autoimmune attack on pancreatic β-cells (1), which leads to a deficiency in insulin secretion and hyperglycemia. Human islet transplantation following the Edmonton protocol has the great potential to treat type 1 diabetic patients. The rate of insulin independence 1 year after islet cell transplantation has significantly improved in recent years (60% at 1 year after transplantation compared with 15% previously) (2). However, at 5 years of follow-up, only approximately 10% of transplanted patients maintain insulin independence (3). The major reason for this limited success is drastic decrease (up to 70%) of β-cell mass of the islet grafts during the first several weeks after transplantation (4,5). Multiple immunological and nonimmunological factors contribute to early graft loss and include allograft rejection, recurrence of autoimmunity, and immunosuppressant toxicity, to name a few (6). In addition, in the absence of established vasculature, lack of nutrients and oxygen supply to the islets results in severe apoptosis. In fact, elevated levels of apoptosis have been shown in pancreatic islets exposed to chronic hyperglycemia immediately after transplantation (7). Therefore, the success of islet transplantation greatly depends on minimizing apoptotic death of the grafts during the first weeks after transplantation (8).

Gene therapy is one strategy aimed at preventing apoptotic islet loss. One of the gene therapy methods for islet transplantation is introducing protective genes into pancreatic islets (e.g., anti-apoptotic genes, genes promoting neovascularization, etc.) (9). An alternative strategy is based on silencing certain genes whose expression is implicated in islet apoptosis. In this study, we investigated the possibility of caspase-3 inhibition by the RNAi mechanism. Caspases are a family of proteases that mediate cell death and are important to the process of cell apoptosis. Caspase-3 is one of the critical downstream effectors that mediate cell apoptosis by both the extrinsic and intrinsic signals pathways (10). Some showed that adenoviral vectors encoding siRNA, targeting the caspase-3 gene, could inhibit apoptosis in insulinoma cells and human islets (11).

Regardless of the specific strategies to minimize β-cell death after transplantation, there is a critical need for islet monitoring using reliable noninvasive methods. In our previous studies, we demonstrated that transplanted pancreatic islets could be followed over time by magnetic resonance imaging (MRI) provided that they were labeled with a suitable contrast agent. Magnetic iron oxide nanoparticles (MN) serve as an excellent contrast agent for monitoring transplanted islets in rodents (12–15) and in nonhuman primates (16). As proof of concept, we showed that small interfering RNA (siRNA) tagged to magnetic nanoparticles could accumulate in pancreatic islets in quantities sufficient for detection by MRI in vitro and for silencing target genes (green fluorescent protein [GFP] was used as a model gene) (17). In our current study, we used a dual-purpose therapy/imaging nanoparticle probe to target the caspase-3 gene. We reason that our "two-in-one" MN-siCaspase-3-imaging probe would silence the apoptotic-related gene, providing significant protection to the grafts from the early loss after transplantation, and at the same time serve as an MRI label to assess the in vivo post-transplant fate of the grafts noninvasively. Our results

From the [1]Molecular Imaging Laboratory, MGH/MIT/HMS Athinoula A. Martinos Center for Biomedical Imaging, Department of Radiology, Massachusetts General Hospital, Harvard Medical School, Boston, Massachusetts; and [2]The Transplantation Biology Research Center, Massachusetts General Hospital, Harvard Medical School, Boston, Massachusetts.
Corresponding author: Anna Moore, amoore@helix.mgh.harvard.edu.
Received 1 October 2010 and accepted 17 November 2010.
DOI: 10.2337/db10-1400

See accompanying commentary, p. 381.

indicated that human islets labeled with the probe showed superior survival after transplantation in mice compared with the islets labeled with parental probe, as demonstrated by in vivo MRI during the initial 2-week period when islet destruction is the most prominent. We believe that these results provide the groundwork for future studies, in which dual-purpose probes could target multiple genes implicated in early graft loss (allo-rejection, islet cell death, autoimmune attack, etc.) with the added benefit of monitoring the (improved) graft outcome.

RESEARCH DESIGN AND METHODS

siRNA. The double-stranded siRNAs targeting human caspase-3 (GenBank accession numbers NM_004346, NM_032991) and scrambled siRNA were designed and synthesized by Dharmacon (Lafatette, CO). The siRNA was modified to incorporate a thiol group on the 5′ end of the sense strand. There was no modification of the antisense strand.

Probe synthesis and characterization. The probe consisted of magnetic nanoparticles (for MRI, synthesized as described in Ref. 20) conjugated to the near-infrared (NIRF) Cy5.5 dye (for correlative microscopy) and to siRNA (for gene silencing) (Fig. 1*A*). The synthesis of the probe involved four distinct steps: synthesis of dextran-coated magnetic nanoparticles (MN), conjugation of the fluorescent dye Cy5.5-*N*-hydroxy succinimide ester to MN, conjugation of the *N*-succinimidyl 3-(2-pyridyldithio) propionate (SPDP) to MN-Cy5.5, and conjugation of siRNA to MN through SPDP linker. In brief, a solution of monoactivated Cy5.5 succinimide ester (Amersham Biosciences, Piscataway, NJ) in 20 mmol/L sodium citrate and 0.15 mol/L NaCl was allowed to react with the previously dialyzed immunopure, amino-derivatized dextran-coated iron oxide (aminated iron oxide, MN-NH_2) at pH 8.5, with constant agitation over a period of 12 h at room temperature. The Cy5.5-labeled aminated iron oxide (MN-NIRF) was purified from unreacted dye using a Sephadex G-25, PD-10 column (Amersham Biosciences). A ratio of 2 Cy5.5 molecules per nanoparticle was obtained. MN-NIRF was then conjugated to the heterobifunctional cross-linker SPDP (Pierce Biotechnology, Rockford, IL) by means of the *N*-hydroxy succinimide ester, followed by purification using a Sephadex G-25, PD-10 column in phosphate-buffered saline (PBS)/EDTA, pH 7.5. The labeling of SPDP per crystal was determined based on the release of pyridine-2-thione at 343 nm ($e = 8.08 \times 10^3\ M^{-1}cm^{-1}$) after the addition of the reducing agent, tris-(2-carboxyethyl) phosphine hydrochloride (TCEP; 35 mmol/L in DMSO). A ratio of 31 SPDP molecules per nanoparticle was obtained.

The caspase-3-targeting and scrambled siRNA duplexes were then conjugated to MN-Cy5.5-SPDP through its 5′-sense thiol group. Before conjugation, the disulfide protecting group on 5′-disulfide bond was deprotected using TCEP according to the manufacturer's instructions. The double-stranded RNA (dsRNA) was then reacted overnight (4°C) with the previously activated MN-Cy5.5-SPDP product via the SPDP cross-linker in PBS/EDTA, pH 8, followed by purification using a Quick Spin Column G-50 Sephadex Column (Roche Applied Science, Indianapolis, IN). The probes designated MN-siCaspase-3/MN-siSCR (Fig. 1*A*) were next purified using magnetic separation columns as described by the manufacturer (Miltenyi Biotec, Auburn CA). The amount of conjugated siRNA was assayed using agarose gel electrophoresis. To assess siRNA dissociation from the nanoparticles under reducing conditions, the probe was pretreated with 15 mmol/L TCEP for 30 min. The siRNA standard probes, untreated probes, and probes treated with reducing agents were applied on a 2% agarose gel in Tris borate-EDTA buffer (Invitrogen, Carlsbad, CA) at 145 V for 1 h. After electrophoresis, the gel was stained with 0.5 μg/ml ethidium bromide for 30 min and visualized using a Molecular Imager FX scanner (Bio-Rad Laboratories, Hercules, CA). The image was quantitated using the software ImageJ, version 1.43u.

Human islet culture and labeling. Human islets were obtained from the Islet Cell Resource Centers (National Institutes of Health and Juvenile Diabetes Research Foundation). The viability and purity of the islets were both higher

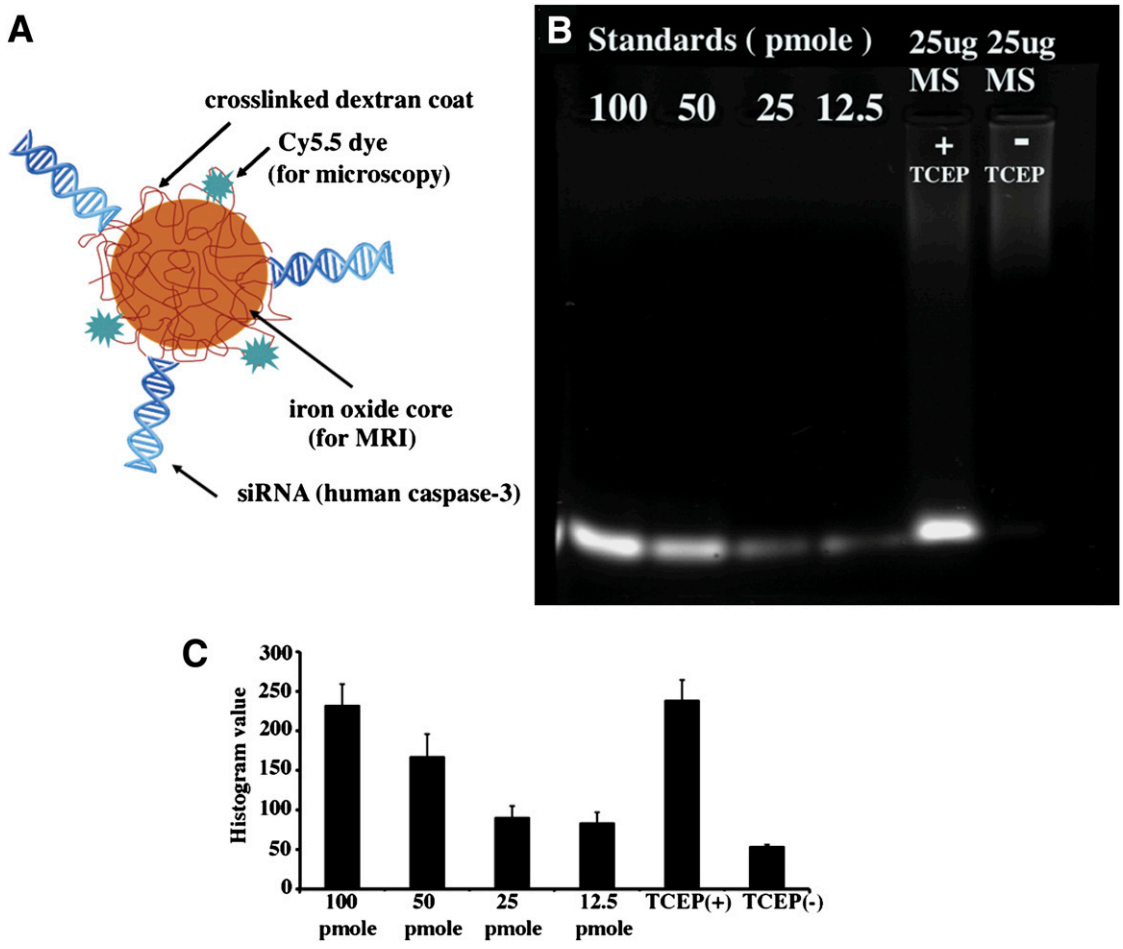

FIG. 1. *A*: Schematic representation of the MN-NIRF-siCaspase-3 probes. *B*: Agarose gel electrophoresis of MN-near-infrared fluorophore-siCaspase-3 probe. *C*: Quantitative analysis showed that 105 pmol siRNA was conjugated to MN-NIRF-siCaspase-3 probe. (A high-quality digital representation of this figure is available in the online issue.)

than 90%. On arrival at our facility, islets were cultured in CMRL-1066 medium (GIBCO, Grand Island, NY) supplemented with 10% FBS and 100 μg/mL penicillin-streptomycin.

For labeling experiments, 1,000 islet equivalents were counted and incubated for 48 h with either MN-siCaspase-3 or MN-siSCR probe in the same medium (0.025 mg Fe, 105 pmol siRNA, in 1 mL medium). To mimic the apoptotic condition, we cultured a group of islets in CMRL-1066 medium supplemented with 100 μg/mL penicillin-streptomycin without serum (serum starvation conditions). After incubation, islets were washed three times in culture medium and used for in vitro and in vivo experiments.

In vitro characterization of labeled islets. Glucose-stimulated insulin secretion was evaluated using static incubation of experimental MN-siCaspase- and control MN-siSCR–labeled islets at low (1.7 mmol/L) and high (20 mmol/L) glucose concentrations. Insulin was measured in supernatants and islet extracts using a human insulin ELISA kit (Mercodia, Uppsala, Sweden). A stimulation index was calculated as the ratio of stimulated to basal insulin secretion normalized by the insulin content.

Islet cell viability was determined after labeling by colorimetric (3-(4,5-dimethylthiazol-2-yl)-2,5-diphenyltetrazolium bromide assay according to the manufacturer's protocol (Promega, Madison, WI). To determine silencing effect after islet treatment with the probes, we performed real-time RT-PCR (TaqMan protocol).

Total RNA was isolated from the experimental and control islets with the RNeasy Mini kit, according to the manufacturer's protocol (QIAGEN, Valencia, CA). The PCR primers and TaqMan probe specific for caspase-3 were designed with Primer Express software 1.5. Primer and probe sequences were as follows: Forward primer, 5′-TGTTCCATGAAGGCAGAGCC-3′; Reverse primer, 5′-TGCGTATGGAGAAATGGGC-3′; and TaqMan Probe 5′-TGGACCACGCAGGAAGGGCCT-3′.

Eukaryotic 18S rRNA TaqMan PDAR Endogenous Control reagent mixture (PE Applied Biosystems, Foster City, CA) was used to amplify 18S rRNA as an internal control, according to the manufacturer's protocol. All samples were run in duplicate.

Caspase-3 protein levels in pancreatic islets were determined by Western blot with rabbit monoclonal antibody to caspase-3 (Abcam, Cambridge, MA) followed by horseradish peroxidase-conjugated goat anti-rabbit antibodies (Cell Signaling Technology, Danvers, MA). Staining of β-actin was used as an internal control. In situ apoptosis detection was performed using transferase-mediated dUTP nick-end labeling (TUNEL) assay (Chemicon, Temecula, CA) according to the manufacturer's protocol. The percentage of cells undergoing apoptosis was calculated from the number of nuclei positive for DNA fragmentation (fluorescein isothiocyanate [FITC] channel) versus the total number of cells present (diaminido phenylindol [DAPI] channel).

Microscopy. Fluorescence microscopy of labeled islets was performed with anticleaved caspase-3 rabbit monoclonal IgG antibody (clone 269518; R&D, Minneapolis, MN) followed by FITC-labeled anti-rabbit IgG (H+L) secondary antibody (Vector Laboratories, Burlingame, CA). Slides were mounted with DAPI-containing mounting medium (Vector Laboratories) and examined under Nikon Eclipse 50i microscope.

For iron staining, we used Prussian Blue stain as described previously (14). All images were acquired using a CCD camera (SPOT 7.4 Slider RTKE; Diagnostic Instruments, Sterling Heights, MI) and analyzed using iVision 4.015 version software.

Islet transplantation. All animal experiments were performed in compliance with institutional guidelines and approved by the Subcommittee on Research Animal Care at Massachusetts General Hospital. MN-siCaspase-3–labeled human pancreatic islets were implanted under the left kidney capsule (1,000 islet equivalents/kidney) of 6-week-old NOD.*scid* mice ($n = 6$). The same number of islets labeled with parental nanoparticles (MN) was transplanted under the right kidney capsule of the same animal.

MRI. Islet phantoms were prepared by fixing islet pellets in 2% paraformaldehyde and sedimenting them in 1% agarose gel. Imaging was performed using a 9.4T AVANCE scanner (Bruker BioSpin, Billerica, MA) equipped with ParaVision 3.0.1 software. The imaging protocol consisted of coronal T2 weighted spin echo (SE) pulse sequences with the following parameters: repetition time (TR)/echo time (TE) = 3,000/8, 16, 24, 32, 40, 48, 56, 64 ms, field of view (FOV) = 3.2 cm^2, matrix size 128, resolution 250 μm^2, and slice thickness = 0.5 mm. Image reconstruction and analysis were performed using Marevisi 3.5 software (Institute for Biodiagnostics, National Research Council, Canada). T2 relaxation times were determined by T2 map analysis of regions of interest drawn around the islet pellets.

In vivo MRI was performed on a 9.4T scanner 1, 3, 5, 7, and 14 days after islet transplantation. The imaging protocols consisted of Multi-Slice Multi Echo T2-weighted map (for volume and T2 relaxivity measurement). Parameters:

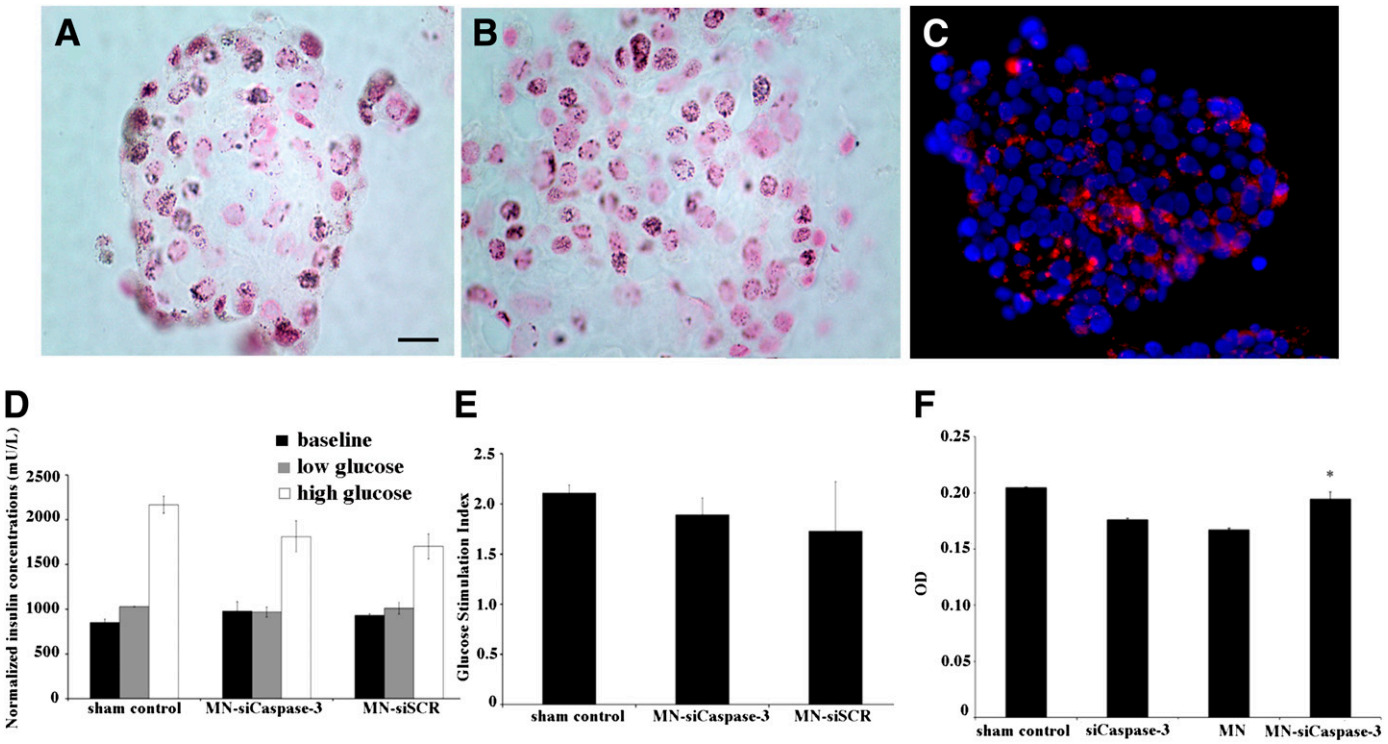

FIG. 2. Prussian Blue staining of the islets treated with MN-siCaspase-3 or MN-NIRF probe. *A*: The islet treated with MN-siCaspase-3 for 48 h. *B*: The islet treated with MN-NIRF-siSCR for 48 h. Prussian Blue staining revealed that approximately 95% of islet cells were labeled with the nanoparticle probes (magnification bar = 10 μm). *C*: Fluorescence microscopy shows islets labeled with MN-siCaspase-3 probe (red, Cy5.5; blue, DAPI nuclear stain). *D*: Insulin release assay of islets incubated with MN-NIRF-siCaspase-3 or control MN-NIRF-siSCR probe for 48 h. *E*: Glucose stimulation index was not significantly different in both treatment groups compared with sham-treated islets ($P > 0.05$). *F*: MTT assay revealed that treatment with siRNA-nanoparticle probes does not cause significant toxicity to islets ($P > 0.05$). (A high-quality digital representation of this figure is available in the online issue.)

TR = 2,000 ms and multiecho TE = 8, 16, 24, 32, 40, 48, 56, and 64; number of averages (NA) = 4; rapid acquisition with relaxation enhancement factor = 8; FOV = 4.4 cm^2, matrix size 128, spatial resolution 312 μm^2, and slice thickness = 0.5 mm. We calculated graft volumes by counting the area in each slice of the region of interest (ROI) outlining the graft and multiplying by the number of slices.

Ex vivo histology. After the last imaging time point, kidneys were removed, fixed in 4% formaldehyde, and embedded in paraffin. Sections were stained for insulin with anti-human insulin antibody (Santa Cruz Biotechnology, Santa Cruz, CA) and for caspase-3 with anticleaved caspase-3 rabbit monoclonal IgG antibody (269518; R&D, Minneapolis, MN). After incubation with Alexa Fluor 594-conjugated secondary goat anti-mouse IgG (H+L; Invitrogen) and FITC-labeled secondary goat anti-rabbit IgG (Vector Laboratories) and counterstaining with DAPI, the sections were used for microscopy as described above. In situ apoptosis detection of kidney sections was performed using TUNEL assay similar to the procedure described above.

Statistical analysis. Data are presented as means ± SD. Statistical differences were analyzed by Student *t* test (SigmaStat 3.0; Systat Software, Richmond, CA). A value of $P < 0.05$ was considered statistically significant.

RESULTS

Characterization of MN-siCaspase-3 probe. To evaluate the number of siRNA molecules associated with nanoparticles, we performed gel electrophoresis with MN-siCaspase-3 under reducing conditions (Fig. 1*B*). As shown in Fig. 1*C*, semiquantitative analysis indicated that 105 pmol siRNA was conjugated to MN-siCaspase-3 probe containing 25 μg of iron.

The uptake of the probes by human islets was confirmed by staining for iron with Prussian Blue stain. As shown in Fig. 2, *A* and *B*, approximately 95% of islet cells were labeled with MN-siCaspase-3 or MN-SCR probes, which was confirmed with fluorescence microscopy (Fig. 2*C*).

At the same time, insulin secretion of human islets following siRNA probe treatment was unaffected in both the experimental and control groups compared with nonlabeled (sham) islets. Glucose stimulation index was not significantly different in all treatment groups (Fig. 2*D* and *E*; $P > 0.05$). MTT assay performed on labeled islets showed that the treatment with the probes did not have any significant effect on islet viability (Fig. 2*F*; $P > 0.05$).

To evaluate the protective effect of siRNA probes, we created treatment conditions where caspase-3 level in the islets was upregulated. We incubated islets without serum (serum starvation), treated them with the probes, and measured caspase-3 mRNA expression by RT-PCR. As shown in Fig. 3*A*, caspase-3 mRNA expression was significantly reduced by the protective action of the MN-siCaspase-3 probe. Although the islets treated with MN-siSCR probes seemed to show a similar trend, the difference between this treatment and treatment with MN-siCaspase-3 probe was highly significant. It is possible that off-target effects (18) played a role in this phenomenon. To determine the caspase-3 protein expression in islets after treatment with the probes, Western blot of the islet samples was performed. As shown in Fig. 3*B*, the expression of caspase-3 protein decreased in islets treated with MN-siCaspase-3 probe compared with control islet group. Fluorescence microscopy confirmed lower expression of caspase-3 in serum-starved islets treated with MN-siCaspase-3 probe compared with the starved nonlabeled islets or islets labeled with the control MN-siSCR probe (Fig. 3*C*). As a consequence, the level of apoptosis in the serum-starved islets after the treatment with the MN-siCaspase-3 probe was significantly lower than in control islets (Fig. 4*A* and *B*). Together, these results demonstrated that there was a significant protective effect of the siRNA probe in islets after incubation under serum starvation conditions.

Finally, we performed MRI of islet phantoms to prove that incubation with magnetic nanoparticles leads to islet labeling, which would allow for following transplanted islets in vivo. Indeed, labeled islets revealed a significant drop in the T2 relaxation times after incubation with

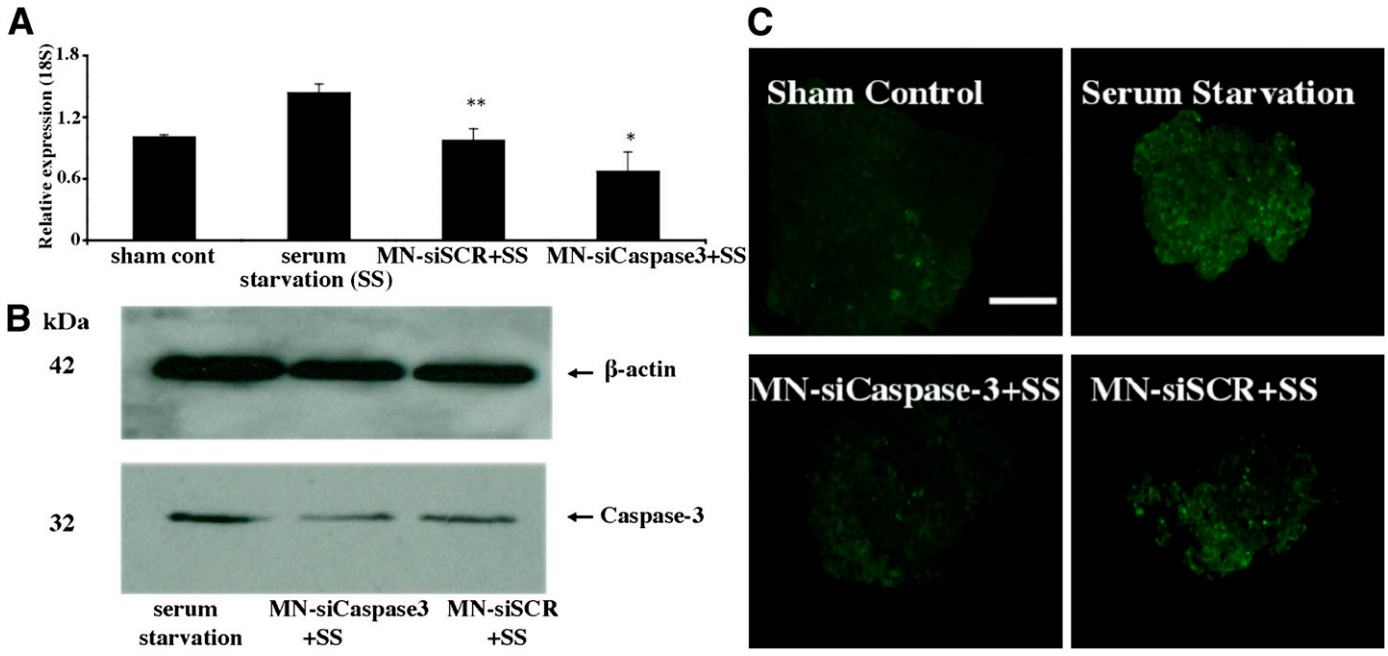

FIG. 3. *A*: Real-time semiquantitative RT-PCR of human caspase-3 expression in islets treated with serum starvation and incubated with MN-siCaspase-3 or the control MN- siSCR probe for 48 h (*$n = 4, P < 0.05$ compared with sham control; **$n = 4, P < 0.05$ compared with MN-siCaspase-3+SS). *B*: Western blot showing decreased level of caspase-3 protein in MN-siCaspase-3–treated islets. *C*: Fluorescence microscopy confirmed that under serum starvation condition, the caspase-3 expression in MN-siCaspase-3–treated islets was decreased compared with islets treated with control probe or serum-starved untreated islets (magnification bar = 50 μm). (A high-quality digital representation of this figure is available in the online issue.)

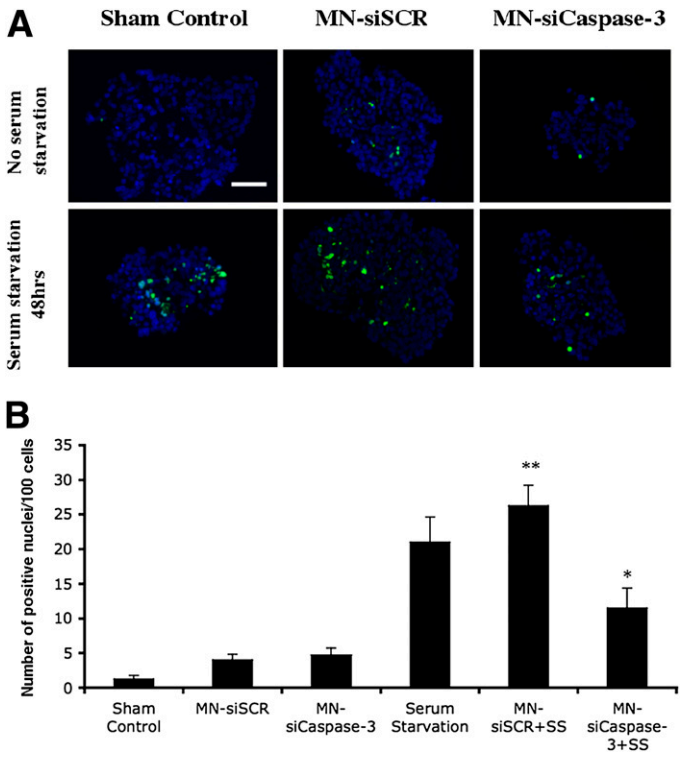

FIG. 4. *A*: **TUNEL assay of the islets incubated in the condition of serum starvation and treated with either MN-siCaspase-3 or MN-siSCR probe for 48 h (magnification bar = 50 μm).** *B*: **Quantitation of TUNEL assay reveals significantly higher level of apoptosis in serum-starved islets treated with the control MN-siSCR probe compared with islet treated with MN-siCaspase-3 probe (*n = 4, P < 0.05 compared with serum starvation-treated islets; **n = 4, P > 0.05 compared with sham-treated islets). (A high-quality digital representation of this figure is available in the online issue.)**

MN-siCaspase-3 or parental nanoparticles compared with unlabeled islets ($P < 0.05$, Fig. 5*A* and *B*).

In vivo MRI of labeled islets. To test our hypothesis that prelabeling with the magnetic siRNA-nanoparticle probe would lead to improved protection and better outcome of islet grafts, we compared the survival properties of human islet grafts labeled with MN-siCaspase-3 and control parental nanoparticles (MN) using in vivo MRI. MN-siCaspase-3–labeled islets were transplanted under the left kidney capsule, and MN-labeled islets were transplanted under the right kidney capsule, so each mouse served as its own control. As shown in Fig. 6*A*, on T2-weighted MR images, transplanted islet grafts underneath the renal capsule appeared as pockets of signal loss disrupting the contour of both kidneys. ROI analysis performed over time revealed that the graft volume decreased both in experimental and control groups. However, this decrease was significantly lower in the animals transplanted with MN-siCaspase-3–labeled islets and was especially pronounced on days 7 and 14 after transplantation (Fig. 6*B*, $P < 0.05$). These results correlated with ex vivo histology, which showed reduced expression of caspase-3 in MN-siCaspase-3–treated grafts (Fig. 6*C*). On the other hand, insulin expression was visibly increased in these grafts compared with controls. This result, in turn, was in accordance with TUNEL staining, which revealed higher apoptosis levels in control grafts (Fig. 6*D*). These data attest to the feasibility of the MN-siCaspase-3 probe to create a protective effect for pancreatic islets after transplantation.

DISCUSSION

Islet transplantation can provide type 1 diabetic patients with improved glycemic control and insulin independence. However, a substantial proportion of the transplanted islet mass fails to engraft because of death by apoptosis. A variety of approaches have been explored to prevent apoptotic destruction of islets in the experimental setting. They include a series of pan-caspase inhibitors and virus mediated anticaspase gene therapy (10,11). Major concerns regarding these approaches deal with poor selectivity and specificity of the inhibitors and the safety of viral vectors. In this study, we demonstrate for the first time that combined siRNA gene therapy and noninvasive imaging can create protection for the graft, reduce apoptosis, and improve the survival properties of the islets in vitro and in vivo.

Programmed cell death is a cascade of events leading to the upregulation of the caspase family. Hypoxia, oxidative damage, serum starvation, inflammatory cytokines (tumor necrosis factor-α, interleukin-1β, γ-interferon, etc.), and other chemical factors (staurosprine, etoposide, cytochrome *c*, etc.) can induce apoptosis in the islet (19,20). Here we showed that serum starvation-induced apoptosis leads to increased caspase activity in the islets. Because activation of the precursor caspase-3 is the converging point of apoptosis, we used the MN-siCaspase-3 probe to label islets to determine whether caspase-3 gene silencing can block apoptosis induced by serum starvation in vitro.

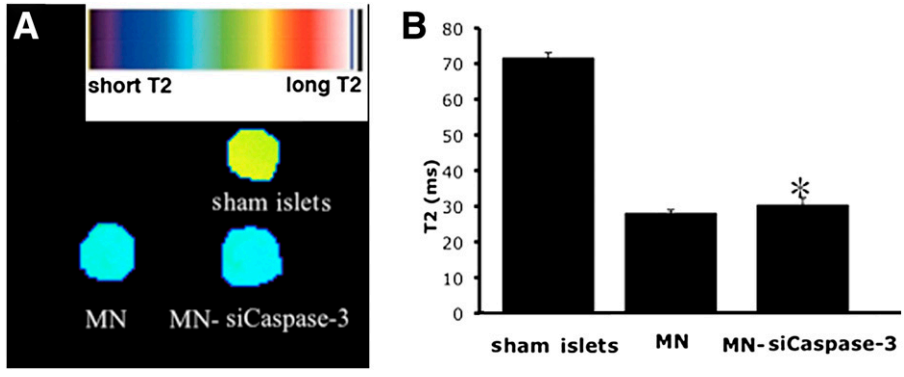

FIG. 5. *A*: **MR images of islet phantoms revealed a decrease in signal intensity after labeling with either MN or MN-siCaspase-3 compared with unlabeled (sham) islets.** *B*: **T2 relaxation times of islet phantoms. (A high-quality digital representation of this figure is available in the online issue.)**

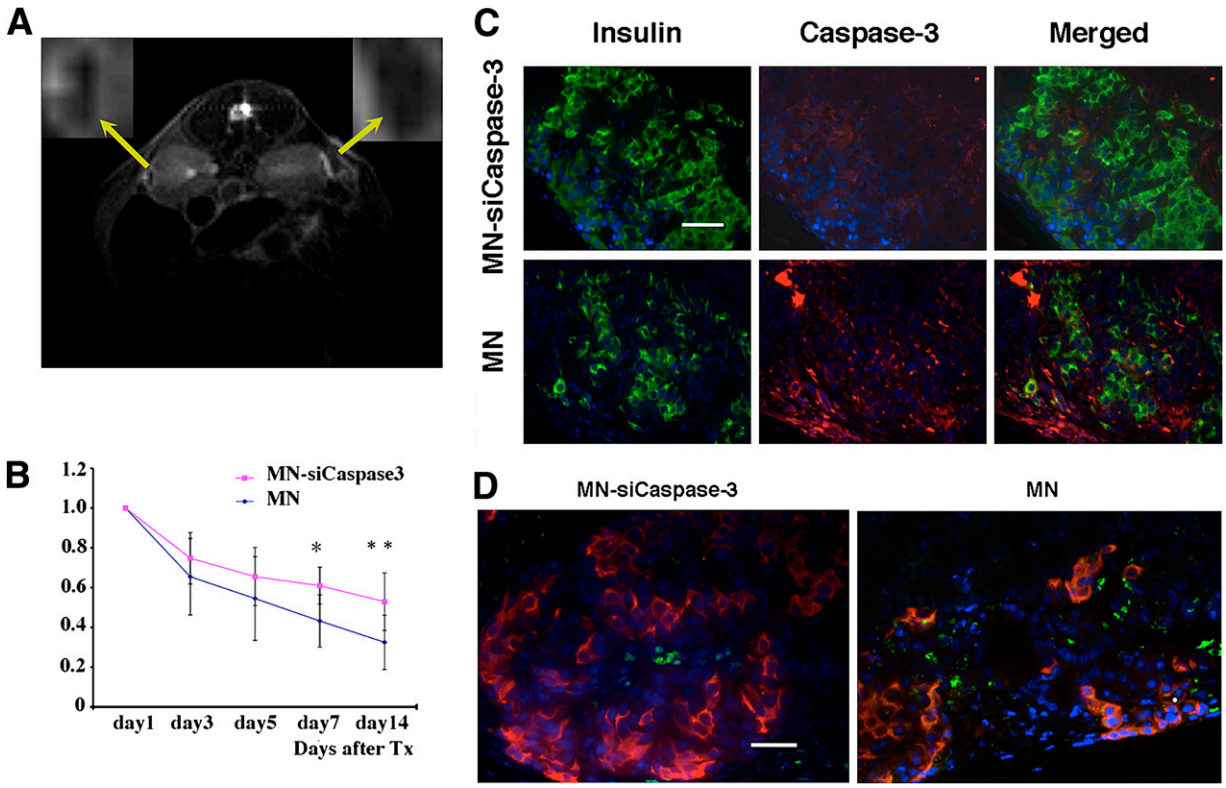

FIG. 6. ***A*****: Representative in vivo MRI of islet transplantation showing MN-siCaspase-3–treated islets implanted under the left kidney (*inset*) and parental MN-treated islets implanted under the right kidney. The dark area outlined under the both kidney capsules represents the labeled grafts (day 3 shown).** ***B*****: Semiquantitative assessment of the relative changes in graft volumes revealed protective effect in MN-siCaspase-3–labeled grafts (*day 7,** $P < 0.05$**; **day 14,** $P < 0.05$**).** ***C*****: Fluorescence microscopy revealed higher expression of insulin and lower expression of caspase-3 in MN-siCaspase-3–treated grafts compared with MN-labeled islet grafts on the 14th day post-transplantation (Tx) (green, insulin; red, cleaved caspase-3; blue, DAPI nuclear stain) (magnification bar = 50 μm).** ***D:*** **TUNEL assay on insulin-stained sections confirmed lower apoptotic rate and higher insulin expression in islets treated with MN-siCaspase-3 compared with islets treated with MN on the 14th day post-Tx (red, insulin; green, TUNEL; blue, DAPI nuclear stain) (magnification bar = 50 μm). (A high-quality digital representation of this figure is available in the online issue.)**

Our data demonstrated that transfection of islets with MN-NIRF-siCaspase-3 reduced caspase-3 mRNA transcripts by 50% under serum starvation. Caspase-3 precursor protein was also significantly suppressed as determined by Western blotting 48 h after incubation.

Our in vivo MRI studies showed that the area of the graft treated with the MN-siCaspase-3 probe was significantly higher than the control islet graft under the renal capsule 7 days and 14 days after transplantation. These data also demonstrate that during the first week after transplantation, there were no differences in reduction of the graft volume between the control and MN-siCaspase-3 groups. Analysis of T2 maps showed that there was no significant change in T2 relaxation times between MN-siCaspase-3 and control groups within 2 weeks. This observation indicated a relative stability of the label within the graft in both experimental and control kidneys during the post-transplant period, which was consistent with our previous report (12).

Because immune rejection could induce apoptosis in the grafts and interfere with the results, all of the in vivo experiments were performed in immunocompromised mice. We propose experiments in diabetic immunocompetent mice transplanted with MN-siRNA–labeled pancreatic islets in the future.

In summary, our data show the feasibility of two-in-one combination of siRNA gene protection therapy and in vivo MRI-noninvasive monitoring of transplanted human islets in mice. We believe that our dual purposes of nanoparticles in addition to delivering siRNA to pancreatic islets offer the added benefit of monitoring grafts in early post-transplant period.

ACKNOWLEDGMENTS

This study was supported by National Institutes of Health [Grant 5R01-DK080784] (to A.M.).

No potential conflicts of interest relevant to this article were reported.

P.W. performed the in vitro experiments, animal surgery, and MRI scanning and participated in the writing of the manuscript. M.V.Y. synthesized the probe. Z.M. participated in the experimental design. L.W. and C.S. participated in the animal studies. G.D. participated in the MRI scanning. A.M. conceived the idea of the project and wrote the manuscript.

REFERENCES

1. Kim MS, Polychronakos C. Immunogenetics of type 1 diabetes. Horm Res 2005;64:180–188
2. Fiorina P, Shapiro AM, Ricordi C, Secchi A. The clinical impact of islet transplantation. Am J Transplant 2008;8:1990–1997
3. Ryan EA, Paty BW, Senior PA, et al. Five-year follow-up after clinical islet transplantation. Diabetes 2005;54:2060–2069
4. Davalli AM, Ogawa Y, Ricordi C, Scharp DW, Bonner-Weir S, Weir GC. A selective decrease in the beta cell mass of human islets transplanted into diabetic nude mice. Transplantation 1995;59:817–820

5. Barshes NR, Wyllie S, Goss JA. Inflammation-mediated dysfunction and apoptosis in pancreatic islet transplantation: implications for intrahepatic grafts. J Leukoc Biol 2005;77:587–597
6. Emamaullee JA, Shapiro AM. Factors influencing the loss of beta-cell mass in islet transplantation. Cell Transplant 2007;16:1–8
7. Biarnés M, Montolio M, Nacher V, Raurell M, Soler J, Montanya E. Beta-cell death and mass in syngeneically transplanted islets exposed to short- and long-term hyperglycemia. Diabetes 2002;51:66–72
8. Moritz W, Meier F, Stroka DM, et al. Apoptosis in hypoxic human pancreatic islets correlates with HIF-1alpha expression. FASEB J 2002; 16:745–747
9. Emamaullee JA, Shapiro AM. Interventional strategies to prevent beta-cell apoptosis in islet transplantation. Diabetes 2006;55:1907–1914
10. Emamaullee JA, Stanton L, Schur C, Shapiro AM. Caspase inhibitor therapy enhances marginal mass islet graft survival and preserves long-term function in islet transplantation. Diabetes 2007;56:1289–1298
11. Cheng G, Zhu L, Mahato RI. Caspase-3 gene silencing for inhibiting apoptosis in insulinoma cells and human islets. Mol Pharm 2008;5:1093–1102
12. Evgenov NV, Medarova Z, Dai G, Bonner-Weir S, Moore A. In vivo imaging of islet transplantation. Nat Med 2006;12:144–148
13. Medarova Z, Evgenov NV, Dai G, Bonner-Weir S, Moore A. In vivo multimodal imaging of transplanted pancreatic islets. Nat Protoc 2006;1:429–435
14. Evgenov N, Medarova Z, Pratt J, et al. In vivo imaging of immune rejection in transplanted pancreatic islets. Diabetes 2006;55:2419–2428
15. Evgenov NV, Pratt J, Pantazopoulos P, Moore A. Effects of glucose toxicity and islet purity on in vivo magnetic resonance imaging of transplanted pancreatic islets. Transplantation 2008;85:1091–1098
16. Medarova Z, Vallabhajosyula P, Tena A, et al. In vivo imaging of autologous islet grafts in the liver and under the kidney capsule in non-human primates. Transplantation 2009;87:1659–1666
17. Medarova Z, Kumar M, Ng SW, et al. Multifunctional magnetic nanocarriers for image-tagged SiRNA delivery to intact pancreatic islets. Transplantation 2008;86:1170–1177
18. Lin X, Ruan X, Anderson MG, et al. siRNA-mediated off-target gene silencing triggered by a 7 nt complementation. Nucleic Acids Res 2005;33:4527–4535
19. Emamaullee JA, Shapiro AM, Rajotte RV, Korbutt G, Elliott JF. Neonatal porcine islets exhibit natural resistance to hypoxia-induced apoptosis. Transplantation 2006;82:945–952
20. Yin D, Ding JW, Shen J, Ma L, Hara M, Chong AS. Liver ischemia contributes to early islet failure following intraportal transplantation: benefits of liver ischemic-preconditioning. Am J Transplant 2006;6:60–68